

THE SNS LINAC COMMISSIONING – COMPARISON OF MEASUREMENT AND MODEL*

Dong-o Jeon[#], Oak Ridge National Laboratory, Oak Ridge, TN37831, U.S.A.

Abstract

The Spallation Neutron Source [1] linac commissioning was an excellent opportunity to benchmark the model with the measurement data for a high intensity linac. A new halo formation mechanism due to large beam eccentricity predicted by simulation was confirmed through a series of emittance measurement. Also the phase scan technique and the acceptance scan technique were benchmarked. Commissioning demonstrated the validity of the model and revealed the shortfall of the model.

NEW HALO FORMATION MECHANISM

A new halo generation mechanism was reported in the non-periodic lattices such as the SNS linac MEBT (Medium-Energy Beam-Transport between RFQ and DTL) [2]. It was found that the nonlinear space charge force resulting from large transverse beam eccentricity ~2:1 in the ~1.6-m-long MEBT chopper section shown in the upper plot of Fig. 3 is responsible for halo formation. This MEBT optics is called as “nominal optics”. As a result, the beam distribution develops halo that leads to beam loss and radio activation of the SNS linac. Designing lattices with transverse beam eccentricity close to 1:1 as shown in the bottom plot of Fig. 1 suppresses this kind of halo generation. This optics is called as “round beam optics”. Multiparticle simulations show that the rms emittance in both planes and halo are reduced significantly when the round beam optics is employed [2].

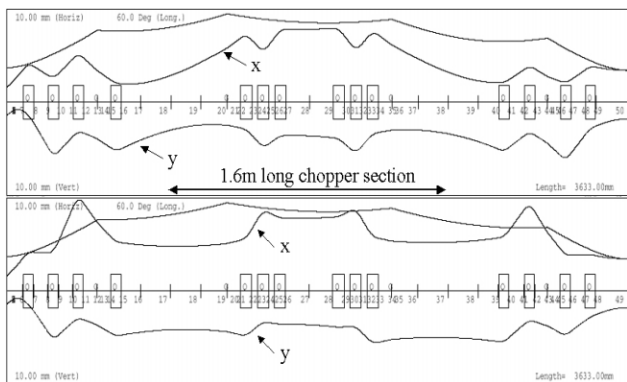


Figure 1: MEBT beam profiles obtained from Trace3D for the “nominal optics” at the top and for the “round beam optics” at the bottom employed for the emittance measurements. The beam is going from left to right.

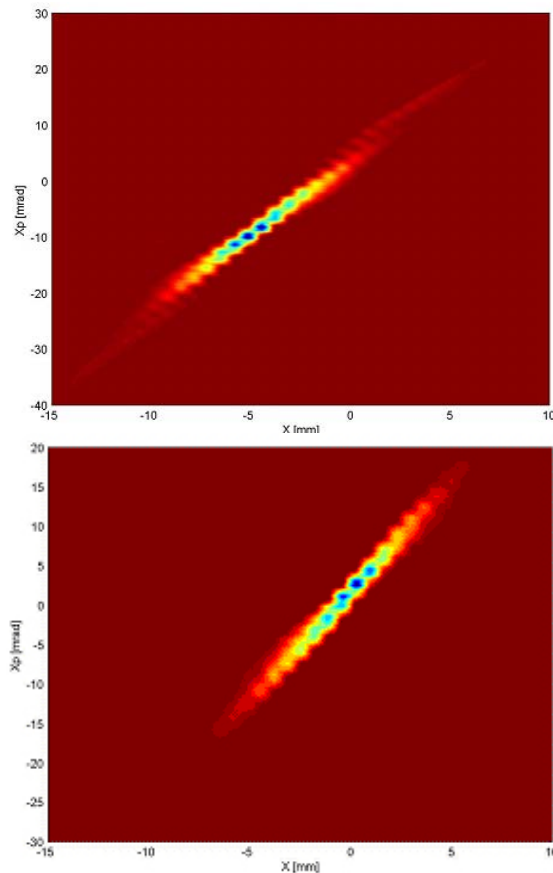


Figure 2: Horizontal emittance plots of the nominal MEBT optics (the top plot) and the round beam optics (the bottom plot). The halo is visibly reduced. The rms emittance is reduced from 0.55 mm-mrad to 0.37 mm-mrad.

Figure 2 shows the results of horizontal emittance measurements for the two different MEBT optics. Compared with the nominal MEBT optics, the halo is visibly reduced and the rms emittance is significantly reduced from 0.55 mm-mrad to 0.37 mm-mrad. Figure 3 shows the results of the vertical emittance measurements. Again visible reduction in the halo should be noted. The rms emittance is reduced from 0.35 mm-mrad to 0.26 mm-mrad. The emittance ratio of $\epsilon(\text{round beam optics})/\epsilon(\text{nominal optics})$ of measurement results are consistent with the multiparticle simulations using the Parmila code [3].

Plots of beam distributions obtained from the Parmila simulation are shown in Fig. 4. The upper plots are beam distributions for the nominal MEBT optics and the lower plots for the round beam optics. The model predicts that the extended halo in the horizontal plane for the nominal optics disappears when the round beam optics is used, just

* SNS is managed by UT-Battelle, LLC, under contract DE-AC05-00OR22725 for the U.S. Department of Energy.
[#]jeond@ornl.gov

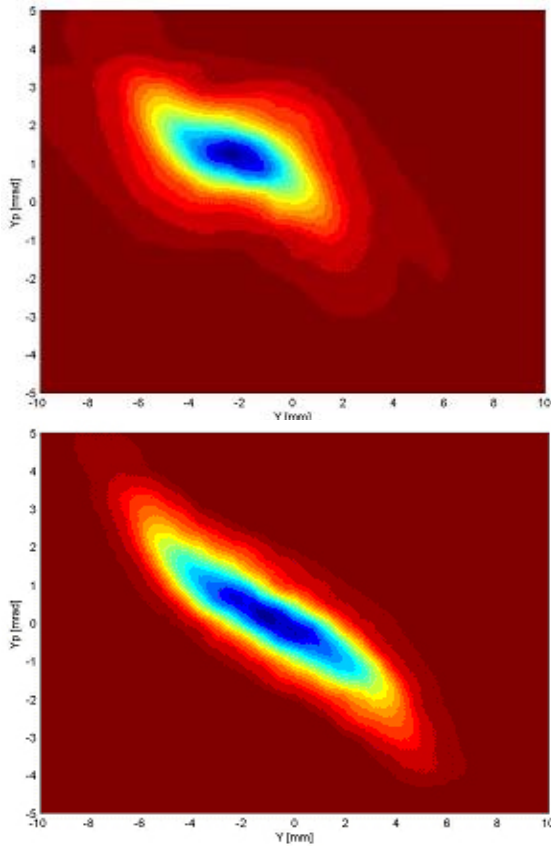


Figure 3: Vertical emittance plots of the nominal MEBT optics (the top plot) and the round beam optics (the bottom plot). The halo is substantially reduced. The rms emittance also is reduced from 0.35 mm-mrad to 0.26 mm-mrad.

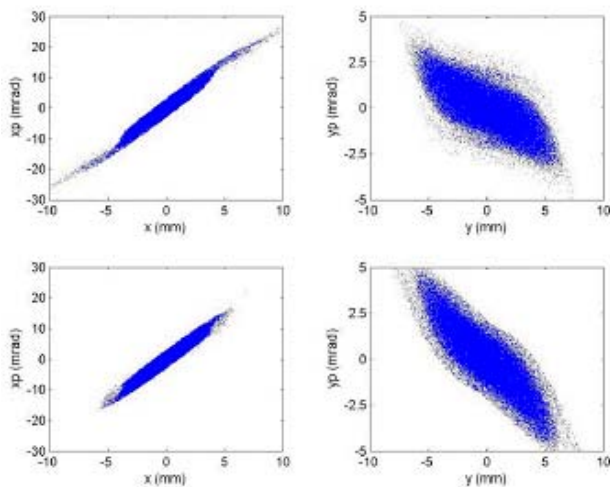


Figure 4: Plots of simulated beam distributions. Upper plots are obtained using the nominal MEBT optics and lower plots using the round beam MEBT optics. Reduction in halo is visible in both planes.

like the measurement results in Fig. 2. The model also predicts that the rms emittance in both planes is reduced significantly when the round beam optics is employed.

The ratio of $\epsilon_x(\text{round beam optics})/\epsilon_x(\text{nominal optics}) = 67\%$ for the measurement and 60% for the simulation. Likewise $\epsilon_y(\text{round beam optics})/\epsilon_y(\text{nominal optics}) = 74\%$ for the measurement and 88% for the simulation.

PHASE SCAN VS. ACCEPTANCE SCAN

Phase Scan (PS) with BPMs

Phase Scan technique is widely used in setting rf set-point of various accelerators and was applied to tuning SNS DTL. The schematic plot of the Phase Scan is in Fig. 5.

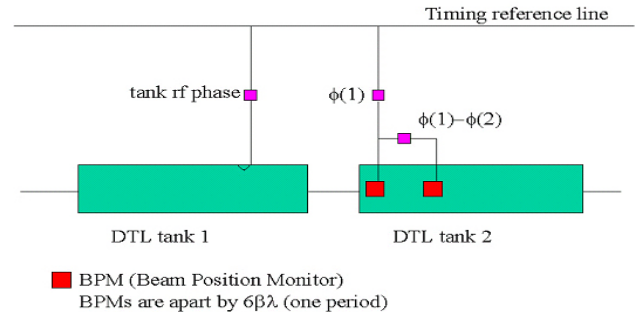


Figure 5: Schematic plot of phase scan with two downstream BPMs.

Comparing simulation and measurements, the rf set-point was obtained. The simulation is based on multiparticle tracking because bunch is relatively long for DTL tanks 1-3. For example, the Full Width Half Maximum of incoming beam bunch length to DTL Tank 1 is about 29° . So it is important to include multiparticle effects to compare with the actual measurements.

Scans were made for three different rf amplitudes for the DTL tank 1 and the results are shown in Fig. 6. Solid circles represent the measurement data for three different rf amplitudes showing the difference of two BPM phase data $\phi(1)-\phi(2)$. Solid lines represent Parmila simulation results. The agreement between the measurement and simulation is excellent. The rf set-point obtained from this phase scan is $(A, \phi)=(0.179, -125.5^\circ)$. Here, “A” is the cavity rf amplitude and “ ϕ ” the cavity rf phase. The incoming beam has an energy deviation of -0.0265 MeV from 2.5 MeV, that is -1.06% .

Phase scan was performed for the DTL tank 2 and the results are shown in Fig. 7. The obtained rf set-point is $(A, \phi)=(0.483, 166.5^\circ)$. The incoming beam has an energy deviation of -0.0236 MeV from 7.523 MeV, that is -0.314% . Now the agreement between the measurement and simulation becomes better.

Phase scan was performed for the DTL tank 3 as shown in Fig. 8, leading to the rf set-point of $(A, \phi)=(0.490, 105.0^\circ)$. The incoming beam has an energy deviation of 0.0579 MeV, that is 0.254% of 22.885MeV.

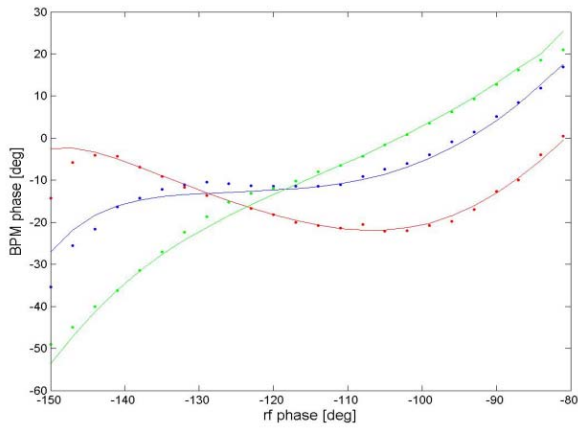


Figure 6: Plots of DTL tank 1 phase scan. Plotted are experimental data (solid circles) and simulation results (solid lines) for three different rf amplitudes.

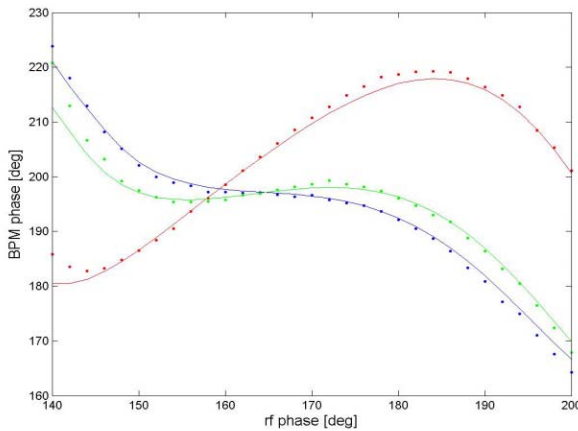


Figure 7: Plots of DTL tank 2 phase scan. Plotted are experimental data (solid circles) and simulation results (solid lines) for three different rf amplitudes.

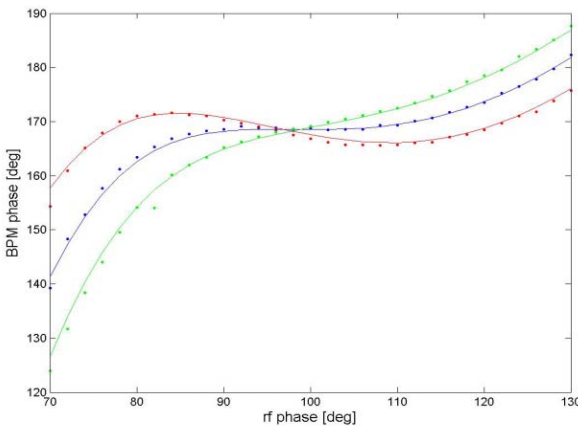


Figure 8: Plots of DTL tank 3 phase scan. Plotted are experimental data (solid circles) and simulation results (solid lines) for three different rf amplitudes.

Acceptance Scan (AS) with ED/FC

Another widely used method for rf set-point is the Acceptance Scan with the Energy Degradar and Faraday

Cup (ED/FC). The ED removes low energy tail of beam bunch and the surviving beam is collected using the FC.

This technique is also based on the multiparticle simulation. For comparison, acceptance scan was performed for DTL tanks 1-3 under the identical conditions. Figure 9 shows the result of DTL tank 1 acceptance scan (top plot) and its derivative (bottom plot), which resulted in an rf set-point of $(A, \phi) = (0.175, -123.9^\circ)$. This is very close to the rf set-point obtained from the Phase Scan.

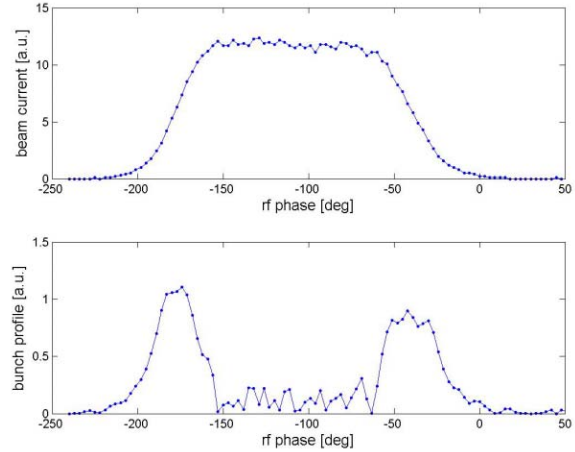


Figure 9: Plot of DTL tank 1 acceptance scan.

Table I summarizes the results of the phase scan and the acceptance scan for the DTL tanks 1-3. The data show an excellent agreement and consistency in both techniques. DTL tank 1 is deemed to be the most sensitive tank of all to tune.

Table I: rf set-point from PS and AS

	Phase scan	Acceptance scan
DTL 1	$(0.179, -125.5^\circ)$	$(0.176, -124.6^\circ)$
DTL 2	$(0.483, 166.5^\circ)$	$(0.484, 168.0^\circ)$
DTL 3	$(0.490, 105.0^\circ)$	$(0.494, 104.7^\circ)$

CONCLUSION

Comparison of the various commissioning data with the model demonstrated that the model is valid and reliable.

REFERENCES

- [1] J. Wei et al, Proceedings of the 2001 Part. Accel. Conf. (Chicago, 2001), p. 319.
- [2] D. Jeon et al, Phys. Rev. ST Accel. Beams **5**, 094201 (2002).
- [3] H. Takeda and J. Stovall, Proceedings of the 1995 Part. Accel. Conf. (Dallas, 1995), p. 2364.